Optical transmission through metal films with a subwavelength hole array in the presence of a magnetic field

Yakov M. Strelniker and David J. Bergman

School of Physics and Astronomy, Raymond and Beverly Sackler Faculty of Exact Sciences, Tel Aviv University, Tel Aviv 69978, Israel

(Received 16 February 1999; revised manuscript received 16 April 1999)

In a recent paper Ebbesen *et al.* [Nature (London) **391**, 667 (1998)] reported on extraordinary optical transmission through periodic hole arrays in metallic films. They explain this by the coupling of light with surface plasmons. Continuing this idea, we have studied such systems in the presence of a static magnetic field. The problem is treated in the quasistatic limit, i.e., when the wavelength is larger than the hole sizes and the array period. We find that the frequency of the transmission peak depends strongly on both the magnitude and the direction of the applied in-plane magnetic field. The directional sensitivity results in a magneto-induced anisotropy of the optical properties of such systems, even for hole arrays with square or triangular symmetry. [S0163-1829(99)51120-X]

Recently it was reported that arrays of submicrometer cylindrical cavities in metal films display highly unusual transmission spectra at wavelengths larger than the array period, when no wavelength sensitive interference should occur.[1,2] These unusual optical properties are apparently due to the coupling of light with plasmons on the surface of the periodically patterned metal film.[1–3] Continuing this idea, we have studied such systems in the presence of a static, in-plane magnetic field $\mathbf{B}_0$. We find that the precise frequencies of the sharp peaks in the transmission spectra depend strongly on the magnitude of $\mathbf{B}_0$, as well as on its direction. The directional sensitivity results in a strong magneto-induced anisotropy of the optical properties. This is similar to the anisotropic magnetoresistance recently found in periodic conducting composites[4–7] and also to the anisotropic macroscopic dielectric properties recently predicted to appear in metal/dielectric composites in the vicinity of a sharp quasistatic resonance.[8] The present discussion is also based upon the quasistatic approximation. In that respect it differs significantly from photonic band discussions of metal/dielectric composites like, e.g., Ref. 9.

Let us consider a geometry which corresponds to the above-mentioned experiment:[1,2] A metal film, with a square array of identical perpendicular cylindrical holes, is placed in a static, in-plane magnetic field $\mathbf{B}_0$ directed along the principal axis *z*. A monochromatic light beam, of angular frequency ω, impinges upon this film along the perpendicular axis *y*, with linear polarization along the principal axis *x* of the array—see Fig. 1(a). The local a.c. permittivity tensor $\hat{\varepsilon}$ of the metal can be written as[8]

$$\hat{\varepsilon}=\varepsilon_0\hat{I}+i\frac{4\pi}{\omega}\hat{\sigma}=\varepsilon_0\hat{I}+i\omega_p^2\frac{\tau}{\omega}\begin{pmatrix}\frac{1-i\omega\tau}{(1-i\omega\tau)^2+H^2} & \frac{-H}{(1-i\omega\tau)^2+H^2} & 0\\ \frac{H}{(1-i\omega\tau)^2+H^2} & \frac{1-i\omega\tau}{(1-i\omega\tau)^2+H^2} & 0\\ 0 & 0 & \frac{1}{1-i\omega\tau}\end{pmatrix}, \tag{1}$$

where ε_0 is the scalar dielectric constant of the background ionic lattice, $\hat{I}$ is the unit tensor, and where we used the free-electron Drude approximation for the conductivity tensor $\hat{\sigma}$ with $\mathbf{B}_0\|z$. The magnetic field enters only through the Hall-to-Ohmic resistivity ratio $H\equiv\rho_H/\rho=\sigma_{xy}/\sigma_{xx}=\mu|\mathbf{B}_0|=\omega_c\tau$, where $\omega_c=eB/mc$ is the cyclotron frequency, τ is the conductivity relaxation time, $\omega_p=(4\pi e^2N_0/m)^{1/2}$ is the plasma frequency, N_0 is the charge carrier concentration, μ is the Hall mobility.

Treating the cylindrical holes as dielectric inclusions embedded in a conducting host, we can apply a general approach developed earlier for the discussion of a metal/dielectric composite medium in the quasistatic regime.[4,10] In this approach, we assume that the composite medium occupies the entire volume in between the infinitely conducting plates of a large capacitor, the parallel plates of which are perpendicular to the α axis, along which the static uniform electric field $\mathbf{E}_0^{(\alpha)}=\nabla r_\alpha=\mathbf{e}_\alpha$ is applied. The local electric potential $\phi^{(\alpha)}(\mathbf{r})$ is then the solution of a boundary value problem based upon a partial differential equation that follows from the requirement $\nabla\cdot\hat{\varepsilon}\cdot\nabla\phi=0$, namely,

$$\nabla\cdot\hat{\varepsilon}\cdot\nabla\phi^{(\alpha)}=\nabla\cdot\theta_{inc}\delta\hat{\varepsilon}\cdot\nabla\phi^{(\alpha)},\quad \mathbf{r}\in V, \tag{2}$$

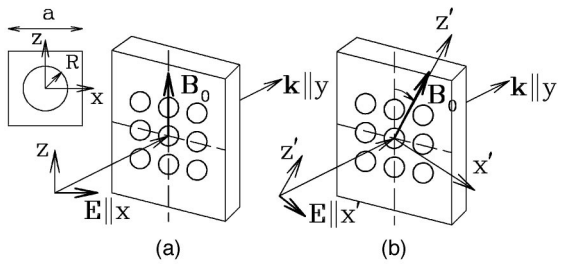

FIG. 1. (a) Schematic drawing of a metal film with a periodic array of holes. The coordinate axes x,y,z are always directed along the principal axes of the simple square lattice, and the applied static magnetic field $\mathbf{B}_0$ always lies in the film plane. The incident light beam is normal to the film surface, i.e., the a.c. electric field $\mathbf{E}$ is parallel to the film plane, while the wave vector is normal to it (i.e., $\mathbf{k}\|y$). Note that the a.c. magnetic field $\mathbf{B}$ of the light wave ($\mathbf{B}\perp\mathbf{E}$) is not important in our considerations and we omit it everywhere. Inset: The $a\times a$ unit cell of the periodic composite film with a cylindrical hole of radius R at its center. (b) The same as (a) but both $\mathbf{B}_0$ and the incident field $\mathbf{E}$ are rotated in the film plane. Here we show the case of transverse polarization $\mathbf{E}\|x'\perp\mathbf{B}_0\|z'$, denoted in the text as $\perp$. The longitudinal polarization $\mathbf{E}\|\mathbf{B}_0\|z'$ is denoted in the text as $\|$.

$$\phi^{(\alpha)}=r_\alpha, \quad \mathbf{r}\in\partial V. \tag{3}$$

Here r_α is the α component of $\mathbf{r}$, $\hat{\varepsilon}_{inc}$ and $\hat{\varepsilon}$ are the electrical permittivity tensors of the inclusions and the host respectively, $\delta\hat{\varepsilon}\equiv\hat{\varepsilon}-\hat{\varepsilon}_{inc}$, $\theta_{inc}(\mathbf{r})$ is the characteristic or indicator function describing the location and the shape of the inclusions ($\theta_{inc}=1$ inside the inclusions and $\theta_{inc}=0$ outside of them). Using a Green function G,

$$G(\mathbf{r},\mathbf{r}'|\hat{\varepsilon})=\frac{1}{4\pi(\varepsilon_{xx}\varepsilon_{yy}\varepsilon_{zz})^{1/2}}\left[\frac{(x-x')^2}{\varepsilon_{xx}}+\frac{(y-y')^2}{\varepsilon_{yy}}+\frac{(z-z')^2}{\varepsilon_{zz}}\right]^{-1/2}, \tag{4}$$

which satisfies Eqs. (2) and (3) with their r.h.s. replaced by 0 and with $V=$ all space, the boundary value problem is transformed into an integrodifferential equation

$$\phi^{(\alpha)}(\mathbf{r})=r_\alpha+\int dV'\,\theta_{inc}(\mathbf{r}')\nabla' G\,\delta\hat{\varepsilon}\cdot\nabla'\phi^{(\alpha)}(\mathbf{r}'). \tag{5}$$

Further progress can be made in the case of a composite medium with a periodic microstructure: We subtract the linear part r_α from the electric potential $\phi^{(\alpha)}$, and expand the remaining periodic part $\psi^{(\alpha)}=\phi^{(\alpha)}-r_\alpha$, as well as the periodic function θ_{inc}, in a Fourier series. This transforms Eq. (5) into an infinite set of linear algebraic equations for the Fourier coefficients $\psi^{(\alpha)}_{\mathbf{g}}=(1/V_a)\int_{V_a}\psi^{(\alpha)}(\mathbf{r})e^{-i\mathbf{g}\cdot\mathbf{r}}dV$, where $\mathbf{g}$ is a vector of the appropriate reciprocal lattice and V_a is the volume of a unit cell. After solving a truncated, finite subset of those equations, corresponding to some maximum reciprocal lattice vector, we can use those Fourier coefficients in order to calculate the bulk effective macroscopic electric permittivity tensor $\hat{\varepsilon}_e$, using the procedure of Ref. 4.

The case of a single inclusion of ellipsoidal or cylindrical shape can be solved exactly when $H=0$.[11] Extensions of that solution for the case $H\neq0$ were evolved in Refs. 10 and 8. Here we invoke an unpublished approach,[12] which was developed originally for d.c. magnetotransport problems, where all the conductivity tensors are real, and which we now extend to a.c. problems, where the permittivity and conductivity tensors are complex.

First we rescale the Cartesian coordinates as follows

$$\xi_1\equiv x/\sqrt{\varepsilon_{xx}}, \quad \xi_2\equiv y/\sqrt{\varepsilon_{yy}}, \quad \xi_3\equiv z/\sqrt{\varepsilon_{zz}}. \tag{6}$$

This greatly simplifies the form of G [see Eq. (4)], which becomes proportional to the Coulomb potential $1/|\boldsymbol{\xi}-\boldsymbol{\xi}'|$. This transformation has a simple geometric interpretation if the rescaling factors are real—that occurs in the d.c. case, when $\hat{\varepsilon}$ is replaced by $\hat{\sigma}$ which is real, and also in the a.c. case if $\omega_p\tau\gg1$, when $\varepsilon_{xx}=\varepsilon_{yy}\cong1-\tau^2\omega_p^2/(\tau^2\omega^2-H^2)$, $\varepsilon_{zz}\cong1-\omega_p^2/\omega^2$. The rescaling then transforms the initial circular cylinder into an elliptic cylinder in $\boldsymbol{\xi}$ space. Differentiating Eq. (5) by $\mathbf{r}$, and rescaling as in Eq. (6), we get

$$E_\alpha(\boldsymbol{\xi})=E_{0\alpha}+\sum_{\beta,\gamma}\frac{1}{(\varepsilon_{\alpha\alpha}\varepsilon_{\beta\beta})^{1/2}}\int_{V_{ell}}d\boldsymbol{\xi}'\frac{\partial}{\partial\xi_\alpha}\times\frac{\partial}{\partial\xi'_\beta}\frac{1}{4\pi|\boldsymbol{\xi}-\boldsymbol{\xi}'|}\delta\varepsilon_{\beta\gamma}E_\gamma(\boldsymbol{\xi}'), \tag{7}$$

where the integration volume V_{ell} in $\boldsymbol{\xi}$ space is the volume of the *transformed inclusion*. We now recall the fact that, if both inclusions and host are isotropic materials and $\mathbf{B}_0=0$, (i.e., $\hat{\varepsilon}_{inc}$, $\hat{\varepsilon}$ are scalar tensors) and if $\mathbf{E}_0$ lies along a principal axis α of an isolated ellipsoidal inclusion, then the electric field inside that inclusion is uniform and points in the same direction, and its magnitude is given by $E_{0\alpha}\varepsilon/[\varepsilon_{inc}n_\alpha+\varepsilon(1-n_\alpha)]$, where n_α is the appropriate depolarization factor (see Ref. 11). Comparing this expression with Eq. (7), it is easy to show that the electric field is uniform inside the inclusions even when $\mathbf{B}_0\neq0$, and that its values there satisfy

$$E_\alpha=E_{0,\alpha}+\frac{n_\alpha(\hat{\varepsilon})}{\varepsilon_{\alpha\alpha}}\sum_\beta\delta\varepsilon_{\alpha\beta}E_\beta, \tag{8}$$

where the coordinate axes are chosen to lie along the principal axes of the transformed inclusion in $\boldsymbol{\xi}$ space. Note that the depolarization factor

$$n_\alpha(\hat{\varepsilon})=\int_{V_{ell}}d\boldsymbol{\xi}'\frac{\partial^2}{\partial\xi_\alpha^2}\frac{1}{4\pi|\boldsymbol{\xi}-\boldsymbol{\xi}'|} \quad \text{for} \quad \boldsymbol{\xi}\in V_{ell} \tag{9}$$

now depends on the precise shape of the transformed inclusion as determined by Eq. (6), therefore it is a function of both H and ω. According to Eq. (6), the cylindrical hole of radius R (with symmetry axis along y) transforms in $\boldsymbol{\xi}$ space into an elliptical cylinder with semi-axes $a=R/\sqrt{\varepsilon_{xx}}$ and $c=R/\sqrt{\varepsilon_{zz}}$. The depolarization factors of the transformed cylinder are

$$n_x=\frac{c}{a+c}=\frac{1}{1+\sqrt{\varepsilon_{zz}/\varepsilon_{xx}}}, \quad n_y=0, \quad n_z=1-n_x. \tag{10}$$

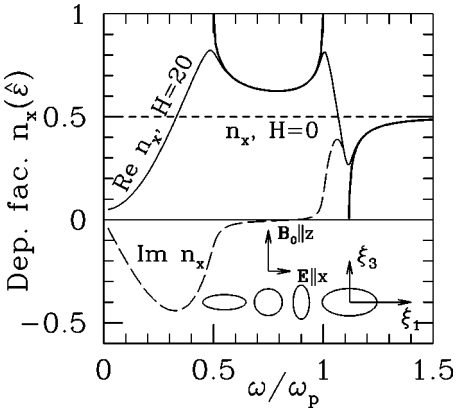

FIG. 2. The depolarization factor $n_x(\hat{\varepsilon})$ plotted vs ω. A horizontal dashed line marks the frequency independent value $n_x=1/2$ for $H=0$. The thick solid line is obtained from Eq. (10) in the limit $\omega_p\tau \gg 1$, for frequencies where $\varepsilon_{zz}/\varepsilon_{xx}$ is real and positive. The thin solid [Re(n_x)] and dashed [Im(n_x)] curves are obtained from Eq. (10) by using the general complex form of the permittivity tensor of Eq. (1). In the lower part there appear schematic drawings of elliptic cylinders in $\boldsymbol{\xi}$ space for different values of ω. The magnetic field $\mathbf{B}_0$ is directed along z (or ξ_3), and $H=20$.

When $H=0$ we have $n_x=n_z=1/2$. However, when $H>0$ these depolarization factors have a complicated dependence on ω, corresponding to the ellipticity of the transformed cylinder (schematic drawings of the cylinder cross section for different ω appear in the lower part of Fig. 2). When the ratio $\varepsilon_{zz}/\varepsilon_{xx}$ is not real and positive, the rescaling transformations of Eq. (6) lose their simple geometric meaning. The depolarization factor $n_x(\hat{\varepsilon})$, which is now a *complex number*, is an analytic continuation of the usual real depolarization factor into the complex plane. Both real and complex values of $n_x(\hat{\varepsilon})$ are shown in Fig. 2 for $H=20$ as functions of ω. We shall see that use of $n_x(\hat{\varepsilon})$ of Eq. (10) in Eq. (14) below gives sensible results at all frequencies [see Figs. 3(a) and 3(b) below]. The possibility to extend the approach of Ref. 12 to the case of complex tensors $\hat{\varepsilon}$ is a significant advantage as compared to other approaches.[13]

Solving the system of linear equations (8), we obtain the following expression for the uniform electric field inside the original circular-cylinder inclusion, for the case where $\mathbf{B}_0 \| z$:

$$\mathbf{E}=\hat{\gamma}\cdot\mathbf{E}_0,$$

$$\hat{\gamma}=\begin{pmatrix} \dfrac{\varepsilon_{xx}}{\varepsilon_{xx}-n_x\delta\varepsilon_{xx}} & \dfrac{n_x\delta\varepsilon_{xy}}{\varepsilon_{xx}-n_x\delta\varepsilon_{xx}} & 0 \\ 0 & 1 & 0 \\ 0 & 0 & \dfrac{\varepsilon_{zz}}{\varepsilon_{zz}-n_z\delta\varepsilon_{zz}} \end{pmatrix}. \tag{11}$$

The bulk effective electric permittivity tensor is defined by (the angular brackets denote a volume average)

$$\hat{\varepsilon}_e\cdot\langle\mathbf{E}(\mathbf{r})\rangle\equiv\langle\hat{\varepsilon}(\mathbf{r})\cdot\mathbf{E}(\mathbf{r})\rangle. \tag{12}$$

For a dilute collection of parallel, circular-cylinder inclusions, it immediately follows that

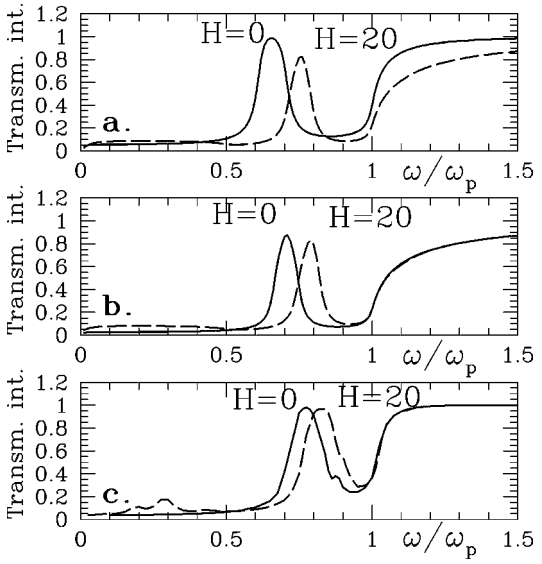

FIG. 3. (a) Transmission coefficient $T_\parallel$ vs frequency ω, along a principal axis of a square array of circular-cylinder holes (i.e., $x\|\mathbf{E}\|\mathbf{B}_0\|z$) with radius-to-lattice-parameter ratio $R/a=0.2$ (i.e., $p_{inc}=0.125$), $\omega_p\tau=40$, $H=0$ (solid line), and $H=20$ (dashed line). Results were calculated using the dilute limit expression for $\varepsilon_{zz}^{(e)}$ similar to Eq. (14). The sharp peaks appear at the surface plasmon resonance frequency of $\varepsilon_{zz}^{(e)}$. (b) Same as (a), but the calculation is now based on a Clausius-Mossotti–type approximation (Refs. 8 and 10). (c) Same as (a), but the calculation used the numerical methods of Ref. 4.

$$\hat{\varepsilon}_e=\hat{\varepsilon}-p_{inc}\delta\hat{\varepsilon}\cdot\hat{\gamma}, \tag{13}$$

where $p_{inc}=V_{inc}/V$ is the volume fraction of the inclusions. The xx component of this,

$$\varepsilon_{xx}^{(e)}=\varepsilon_{xx}\left[1-p_{inc}\frac{\delta\varepsilon_{xx}}{\varepsilon_{xx}-n_x(\hat{\varepsilon})\,\delta\varepsilon_{xx}}\right], \tag{14}$$

will clearly have a resonance when the denominator vanishes. We assume that $\hat{\varepsilon}_{inc}$ is a scalar tensor which is independent of ω and H, and we use Eq. (1) for $\hat{\varepsilon}$. The denominator of Eq. (14) will then vanish whenever ω satisfies the following complex equation

$$\omega^3-i\frac{2}{\tau}\omega^2-\left[\frac{1+H^2}{\tau\omega_p}+\frac{1-n_x(\hat{\varepsilon})}{\zeta}\right]\omega_p^2\omega-i\kappa=0, \tag{15}$$

where $\kappa=[1-n_x(\hat{\varepsilon})]\omega_p^2/\tau\zeta$ and $\zeta=\varepsilon_0-n_x(\hat{\varepsilon})(\varepsilon_0-\varepsilon_{inc})$. Note that this is not a simple cubic equation, since $n_x(\hat{\varepsilon})$ also depends upon ω [see Eq. (10)]. In our subsequent calculations we take $\varepsilon_0=\varepsilon_{inc}=1$, therefore $\zeta=1$, and we also assume $\omega_p\tau\gg1$. For $H=0$ [in that case $n_x=n_z=1/2$ and Eq. (15) is in fact a simple cubic equation], this equation then has a solution which is almost real $\omega_{sp}\cong\omega_p/\sqrt{2}$—that is the usual surface plasmon resonance frequency for a cylindrical inclusion.[14] For $\omega_p\tau>|H|$, the contribution of $n_x(\hat{\varepsilon})$ to the H dependence of ω_{sp} is small compared to the explicit H dependence in this expression. Therefore, the surface plasmon peak in $\varepsilon_{xx}^{(e)}(\omega)$ should move up to higher frequencies with increasing $|H|$. This behavior is qualitatively similar to what

was found in Refs. 8 and 15 where the converse type of composite configuration was studied, i.e., metallic inclusions inside a dielectric host.

In Fig. 3(a) we show the longitudinal transmission coefficient $T_{\parallel}(\omega)$ when $\mathbf{E}$ lies along a principal axis of a dilute hole array [i.e., $\mathbf{E}\|\mathbf{B}_0\|z$, $R/a=0.2$—see Fig. 1(a)] calculated using Eq. (14), for $H=0$ and $H=20$. The same quantities were also calculated using a Clausius-Mossotti–type approximation,[10,8] and using the numerical methods of Ref. 4. Those results are shown in Figs. 3(b) and 3(c), respectively, and are in reasonable agreement with the dilute limit results of Fig. 3(a). The sharp peaks occur near the magnetic-field-dependent surface plasmon resonance frequency of $\varepsilon_{zz}^{(e)}$.

In the system under discussion here, since the host is a conductor, we expect a strong dependence of $\hat{\sigma}_e(\mathbf{B}_0)$, and therefore also of $\hat{\varepsilon}_e(\mathbf{B}_0)$, on the direction of $\mathbf{B}_0$, similar to what was found previously in the d.c. case.[4–7] However, anisotropy of this kind cannot appear in the simple low density or Clausius-Mossotti–type approximations described above. Therefore, in order to look for such behavior in the magneto-optical properties, we had to use the numerical methods of Ref. 4. In this way, we were able to calculate the angular profiles of both the real and imaginary parts of $\hat{\varepsilon}_e$, for the case where the magnetic field $\mathbf{B}_0$ is rotated in the film plane, as shown in Fig. 1(b). These results are somewhat similar to what was found earlier for a composite where a periodic array of metal inclusions are embedded in a dielectric host.[8] Using those results, we calculated the angular profiles of the optical transmission coefficients for such a film—those are shown in Fig. 4.

In summary, we have shown that the position of the peak in the extraordinary optical transmission, recently reported in Ref. 1, should depend not only on the plasma frequency, but also on the magnitude of an applied static magnetic field $\mathbf{B}_0$, as well as on its direction. This dependence should be strongest in the case of a highly doped semiconducting film: In that case, it is possible to obtain large values of the Hall mobility μ, and therefore also large values of the dimensionless magnetic field $H=\mu|\mathbf{B}_0|$. The value of $\omega_p\tau$ in this case can be of the same order of magnitude as in conventional metals (in our calculations we assumed $\omega_p\tau=40$, while for a typical free-electron metal like Al we have $\omega_p\tau\approx 100$). Thus such anisotropic, magnetic-field-dependent, extraordinary optical transmission, in the infrared range of frequencies, can be sought in heavily doped semiconductor films with an array of holes with a submicron periodicity. In transition metal films of Ag or Au, where surface plasmons are easily observed in visible light, stronger magnetic fields would be needed in order to observe the behavior described here. The detailed treatment would also require going beyond the quasistatic approximation.

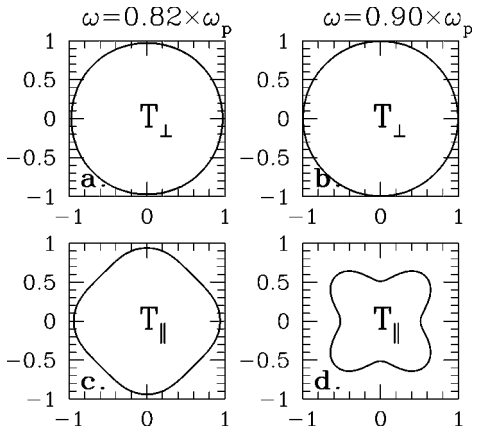

FIG. 4. Polar plots of the transmission coefficients $T_{\perp}$ and $T_{\parallel}$, obtained using the bulk effective electric permittivity tensor $\hat{\varepsilon}^{(e)}$, calculated numerically for a thin metallic film with a periodic square array (see Fig. 1) of cylindrical holes with radius-to-lattice-parameter ratio $R/a=0.2$, when a static magnetic field $\mathbf{B}_0$ is rotated in the film plane. The subscript ''$\perp$'' corresponds to the polarization $\mathbf{E}\perp\mathbf{B}_0$, while the subscript ''$\|$'' corresponds to the polarization $\mathbf{E}\|\mathbf{B}_0$. The field $\mathbf{B}_0$ has a fixed magnitude, corresponding to $H=20$, the angular frequencies of the applied electric field are $\omega=0.82\omega_p$ [(a) and (c)] and $\omega=0.9\omega_p$ [(b) and (d)], and $\omega_p\tau=40$.

This research was supported in part by grants from the U.S.–Israel Binational Science Foundation, the Israel Science Foundation, the Tel Aviv University Research Authority, and the Gileadi Fellowship program of the Ministry of Absorption of the State of Israel.

[1] T. W. Ebbesen, H. J. Lezec, H. F. Ghaemi, T. Thio, and P. A. Wolff, Nature (London) **391**, 667 (1998).
[2] H. F. Ghaemi, T. Thio, D. E. Grupp, T. W. Ebbesen, and H. J. Lezec, Phys. Rev. B **58**, 6779 (1998).
[3] U. Schröter and D. Heitmann, Phys. Rev. B **58**, 15 419 (1998).
[4] D. J. Bergman and Y. M. Strelniker, Phys. Rev. B **49**, 16 256 (1994).
[5] M. Tornow, D. Weiss, K. v. Klitzing, K. Eberl, D. J. Bergman, and Y. M. Strelniker, Phys. Rev. Lett. **77**, 147 (1996).
[6] D. J. Bergman and Y. M. Strelniker, Phys. Rev. Lett. **80**, 3356 (1998).
[7] D. J. Bergman and Y. M. Strelniker, Phys. Rev. B **59**, 2180 (1999).
[8] D. J. Bergman and Y. M. Strelniker, Phys. Rev. Lett. **80**, 857 (1998).
[9] V. Kuzmiak and A. A. Maradudin, Phys. Rev. B **55**, 7427 (1997).
[10] D. Stroud, Phys. Rev. B **12**, 3368 (1976).
[11] L. D. Landau, E. M. Lifshitz, and L. P. Pitaevskii, *Electrodynamics of Continuous Media* (Pergamon Press, Oxford, 1984).
[12] D. J. Bergman (unpublished).
[13] J. B. Sampsell and J. C. Garland, Phys. Rev. B **13**, 583 (1976).
[14] H. Raether, *Surface Plasmons* (Springer-Verlag, Berlin, 1988).
[15] G. Dresselhaus, A. F. Kip, and C. Kittel, Phys. Rev. **98**, 368 (1955).